Design Aspects of Single-Angle Members

PIERRE DUMONTEIL

Abstract

Used since the very beginning of steel construction, single-angle members are found in many different kinds of structures. Nearly all single-angle members are eccentrically loaded in some fashion, yet truss chords, tower legs and similar members not carrying transverse loads are usually designed as centrally loaded members. ANSI/AISC 360-05, *Specification for Structural Steel Buildings,* prescribes complex design calculations for eccentrically loaded single angles, but also provides simplified equations that adjust the *KL/r* ratio to account for eccentricities and end restraints. The purpose of this paper is to examine the possibility of simpler calculations and to explore the behavior of single-angle members.

Keywords: single angles, eccentric loads, lateral-torsional buckling, steel construction.

INTRODUCTION

Whether hot-rolled or cold-formed, angles are among the simplest steel shapes. Their shape affords simple connections with other angles or other shapes. Used since the very beginning of steel construction, single-angle members are found in many different kinds of structures: roof trusses, power transmission towers, conveyor trusses, etc.

Nearly all single-angle members are eccentrically loaded in some fashion or another. Even so, truss chords, tower legs, or similar members that do not carry transverse loads are traditionally designed as centrally loaded members. For eccentrically loaded single angles in general, the ANSI/AISC 360-05 specification (also referenced as the AISC *Specification* in this paper) prescribes design calculations that are undoubtedly complicated and tedious. Fortunately, AISC 360-05 follows the example of the ASCE Standard 10-90 and provides for most truss web members simple formulae that adjust the *KL/r* ratio to account for eccentricities and end restraints. The purpose of this paper is to examine whether simpler calculations are possible and to explore to some extent the behavior of single-angle members.

POINTS OF CONSIDERATION: FIVE OR THREE?

The first decision facing the designer is at which specific points in the section or "points of consideration" the combined stress should be computed. ANSI/AISC 360-05 is silent on this matter.

Pierre Dumonteil, retired licensed Professional Engneer, 6887 E. Long Ave, Englewood, CO, 80112. E-mail: pey.dumonteil@comcast.net

The elastic section moduli S_w and S_z relative to the principal axes are not listed in the AISC *Steel Construction Manual*, in which the section properties of structural steel angles are calculated on the simple assumption that the cross-section consists of two rectangles. If this model were geometrically exact, it would be theoretically necessary to consider the elastic section moduli at the five salient corners, numbered 1 to 5 on Figure 1a. This has been proposed by Yongcong Ding and M.K.S. Madugula (2004), who also included tables of moduli S_w and S_z for the steel angles listed in the AISC *Manual*. A different point of view is that of Lutz (1996) and Sakla (2001), who base their calculations on three points only, numbered 1 to 3 on Figure 1c. Why some experts use three points and others five is certainly a valid question, on which the following comments are offered.

1. The actual cross-section is that shown on Figure 1b. While there are no standards governing the fillet radii at the tips, it is a fact that the inside tips are always rounded. In practice, Points 3 and 4 of Figure 1a do not exist.

2. The stipulation of a nominal bending strength $M_n = 1.5M_y$ for compact angles implies a very substantial amount of plastic flow, essentially at the leg tips. The actual stress

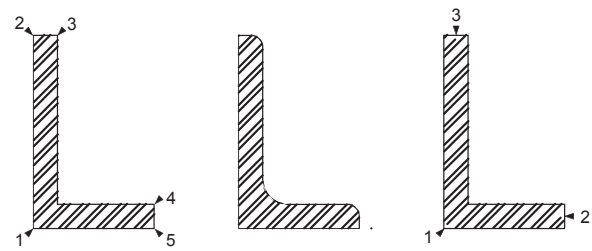

(a) Simplified Geometry, 5 Salient Corners (b) Actual Geometry with Fillets (c) Proposed Points of Consideration

Fig. 1. Geometry and points of consideration.

distribution is further complicated by residual stresses, which, at the tips, are compressive and may reach 0.25 times the yield stress (ECCS, 1976). As the angle reaches the limit state of yielding, the stress distribution in the vicinity of the toes is nearly uniform, and is probably better described by the stresses at Points 2 and 3 of Figure 1c.

3. For noncompact and slender angles, the limit state of local buckling is based on theories that assume a uniform stress across the thickness t of the leg. This is better expressed by the two tips of Figure 1c.

4. The limit state of lateral-torsional buckling applies to the whole cross-section and is not related to specific points in the section.

5. Considering only three points is, of course, simpler and reduces the amount of computation by at least one third. In this respect, the recommendation for equal-leg angles of ANSI/ASCE Standard 10-90 (1992) is noteworthy:

   The following section moduli based on centerline dimensions may be used in lieu of those based on overall dimensions:

$$S_u = \frac{b^2 t}{1.5\sqrt{2}} \qquad S_z = \frac{b^2 t}{3\sqrt{2}}$$

   In the ASCE document, the index u is used instead of the subscript w used in the AISC *Manual*; and the symbol b represents the leg width less half the thickness. Obviously, the ASCE standard wishes to avoid excessive accuracy.

For these reasons, it is strongly believed that the points of consideration should consist only of the three critical points, marked 1, 2 and 3 on Figure 1c. The corner (or heel) of the angle, Point 1, is seldom critical, but that possibility cannot be ruled out entirely.

Section properties could include fillets if their maximum and minimum radii were specified by an industry wide standard. Even so, more complicated calculations for section properties do not seem warranted, particularly in view of items 2 and 5 in the preceding paragraphs. Accordingly, the section moduli and other properties shown in Table 1 are based on the two-rectangle cross-section of Figure 1c.

LATERAL-TORSIONAL BUCKLING ABOUT GEOMETRIC AXES (EQUAL-LEG ANGLES)

Equal-leg angles may be treated either with the general method, based on the principal axes, or with a simpler approach that allows their design using properties about geometric axes. The axis of the applied bending moment must be parallel to one of the legs, as in Figure 2.

In the geometric axis approach, the worst case is that of maximum compression at the toes, in which the elastic lateral-torsional moment M_e is, according to Equation F10-4a:

$$M_e = 0.66\frac{Eb^4 t}{L^2}C_b\left(\sqrt{1+0.78\left(\frac{Lt}{b^2}\right)^2}-1\right) \qquad (1)$$

Letting $\varpi = \dfrac{Lt}{b^2}$, the lateral-torsional moment M_e is

$$M_e = 0.66EC_b t^3\frac{\sqrt{1+0.78\varpi^2}-1}{\varpi^2} = \frac{0.515EC_b t^3}{1+\sqrt{1+0.78\varpi^2}} \qquad (2)$$

This moment must be compared to the yield moment $M_y = 0.80S_xF_y$. For our purpose, a sufficient approximation to S_x is $S_x = \dfrac{b^2 t}{4}$. The nondimensional ratio M_y/M_e is then

$$\frac{M_y}{M_e} \approx 0.388\frac{F_y}{EC_b}\left(\frac{b}{t}\right)^2\left(1+\sqrt{1+0.78\varpi^2}\right) \qquad (3)$$

At this stage, it will be convenient to introduce the notation

$$\gamma = \frac{b}{t}\sqrt{\frac{F_y}{E}} \qquad (4)$$

Equation 3 becomes

$$\frac{M_y}{M_e} \approx 0.388\frac{\gamma^2}{C_b}\left(1+\sqrt{1+0.78\varpi^2}\right) \qquad (5)$$

In accordance with Equation F10-3 of the AISC *Specification*, the ratio of the nominal bending strength M_n to the yield moment M_y is:

$$\frac{M_n}{M_y} = 1.92 - 1.17\sqrt{\frac{M_y}{M_e}} \le 1.5 \qquad (6)$$

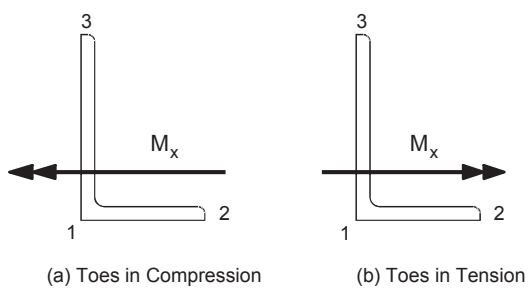

Fig. 2. Bending moment orientation.

Table 1. Section Moduli and Lateral-Torsional Constants of Angle Shapes*											
Angle Shape	I_w (in.^{4})	I_z (in.^{4})	α (deg.)	S_{w1} (in.^{3})	S_{w2} (in.^{3})	S_{w3} (in.^{3})	S_{z1} (in.^{3})	S_{z2} (in.^{3})	S_{z3} (in.^{3})	L_w (in.)	M_{w0} (kip-in.)
L8×8×1⅛	155	40.8	45	–	29.5	29.5	12.0	15.4	15.4	–	–
L8×8×1	141	36.7	45	–	26.6	26.6	11.0	13.8	13.8	–	–
L8×8×⅞	127	32.6	45	–	23.7	23.7	9.93	12.1	12.1	–	–
L8×8×¾	111	28.4	45	–	20.6	20.6	8.81	10.5	10.5	–	–
L8×8×⅝	94.8	24.1	45	–	17.4	17.4	7.62	8.84	8.84	–	–
L8×8×9⁄16	86.3	21.8	45	–	15.8	15.8	6.99	7.99	7.99	–	–
L8×8×½	77.7	19.6	45	–	14.2	14.2	6.34	7.14	7.14	–	–
L8×6×1	98.3	21.2	28.49	63.7	24.8	18.7	7.81	7.61	13.8	18.4	29600
L8×6×⅞	88.3	18.9	28.67	58.2	22	16.7	7.09	6.72	12.1	21.1	20000
L8×6×¾	77.7	16.5	28.84	52.1	19.1	14.6	6.32	5.82	10.4	24.8	12700
L8×6×⅝	66.4	14.0	29.01	45.3	16.2	12.3	5.50	4.92	8.73	30.0	7390
L8×6×9⁄16	60.6	12.7	29.09	41.7	14.7	11.2	5.06	4.45	7.89	33.4	5410
L8×6×½	54.5	11.5	29.16	37.8	13.2	10.1	4.60	3.99	7.04	37.8	3810
L8×6×7⁄16	48.3	10.1	29.24	33.8	11.6	8.88	4.12	3.52	6.19	43.3	2560
L8×4×1	73.4	7.87	13.89	27.1	23.1	14.9	4.51	3.49	11.9	20.0	15200
L8×4×⅞	66.0	7.00	14.18	24.8	20.5	13.2	4.11	3.07	10.3	23.1	10300
L8×4×¾	58.1	6.12	14.45	22.2	17.8	11.6	3.69	2.65	8.75	27.2	6500
L8×4×⅝	49.8	5.23	14.71	19.3	15.1	9.8	3.24	2.24	7.27	33.0	3790
L8×4×9⁄16	45.4	4.77	14.83	17.7	13.7	8.9	3.00	2.03	6.54	36.8	2770
L8×4×½	40.9	4.30	14.95	16.1	12.3	7.99	2.74	1.82	5.82	41.7	1950
L8×4×7⁄16	36.3	3.82	15.07	14.4	10.8	7.05	2.48	1.61	5.11	48.0	1310
L7×4×¾	41.2	5.68	17.94	19.8	13.9	9.22	3.28	2.60	7.28	21.8	7450
L7×4×⅝	35.4	4.85	18.23	17.4	11.8	7.84	2.88	2.19	6.05	26.4	4350
L7×4×½	29.2	3.99	18.50	14.6	9.62	6.40	2.44	1.78	4.85	33.4	2240
L7×4×7⁄16	25.9	3.54	18.63	13.1	8.50	5.66	2.20	1.58	4.26	38.4	1510
L7×4×⅜	22.6	3.09	18.75	11.5	7.35	4.90	1.95	1.36	3.66	45.2	954
L6×6×1	55.9	15.0	45	–	14.4	14.4	5.69	7.65	7.65	–	–
L6×6×⅞	50.5	13.3	45	–	12.8	12.8	5.18	6.73	6.73	–	–
L6×6×¾	44.7	11.6	45	–	11.2	11.2	4.63	5.82	5.82	–	–
L6×6×⅝	38.4	9.87	45	–	9.56	9.56	4.03	4.89	4.89	–	–
L6×6×9⁄16	35.2	8.98	45	–	8.69	8.69	3.72	4.43	4.43	–	–
L6×6×½	31.7	8.07	45	–	7.81	7.81	3.39	3.96	3.96	–	–
L6×6×7⁄16	28.2	7.15	45	–	6.9	6.90	3.04	3.49	3.49	–	–
L6×6×⅜	24.6	6.20	45	–	5.98	5.98	2.67	3.01	3.01	–	–
L6×6×5⁄16	20.8	5.23	45	–	5.03	5.03	2.29	2.53	2.53	–	–

* Refer to Figure 1c for applicable geometry

Table 1. Section Moduli and Lateral-Torsional Constants of Angle Shapes* (cont'd.)											
Angle Shape	I_w (in.^{4})	I_z (in.^{4})	α (deg.)	S_{w1} (in.^{3})	S_{w2} (in.^{3})	S_{w3} (in.^{3})	S_{z1} (in.^{3})	S_{z2} (in.^{3})	S_{z3} (in.^{3})	L_w (in.)	M_{w0} (kip-in.)
L6×4×⅞	31.6	5.87	22.85	20.8	11.8	8.23	3.16	2.94	6.71	13.3	14800
L6×4×¾	28.1	5.13	23.18	18.9	10.3	7.23	2.83	2.54	5.71	15.6	9390
L6×4×⅝	24.2	4.37	23.49	16.7	8.78	6.17	2.49	2.15	4.75	18.9	5480
L6×4×9⁄16	22.2	3.99	23.63	15.4	7.97	5.62	2.3	1.95	4.28	21.1	4020
L6×4×½	20.1	3.59	23.77	14.1	7.16	5.06	2.11	1.75	3.81	23.9	2840
L6×4×7⁄16	17.9	3.19	23.90	12.7	6.33	4.48	1.9	1.54	3.34	27.4	1910
L6×4×⅜	15.6	2.78	24.03	11.2	5.48	3.88	1.68	1.34	2.88	32.2	1210
L6×4×5⁄16	13.2	2.36	24.16	9.63	4.61	3.28	1.45	1.13	2.41	38.9	703
L6×3½×½	18.2	2.6	18.97	10.7	7.02	4.69	1.77	1.35	3.6	24.4	2290
L6×3½×⅜	14.2	2.01	19.27	8.53	5.37	3.6	1.42	1.03	2.71	33.0	975
L6×3½×5⁄16	12	1.71	19.42	7.32	4.52	3.04	1.23	0.871	2.27	40.0	567
L5×5×⅞	28	7.56	45	–	8.67	8.67	3.41	4.64	4.64	–	–
L5×5×¾	24.9	6.59	45	–	7.61	7.61	3.06	4	4	–	–
L5×5×⅝	21.6	5.6	45	–	6.5	6.5	2.68	3.37	3.37	–	–
L5×5×½	17.9	4.59	45	–	5.33	5.33	2.26	2.73	2.73	–	–
L5×5×7⁄16	16	4.07	45	–	4.72	4.72	2.04	2.4	2.4	–	–
L5×5×⅜	14	3.54	45	–	4.1	4.1	1.8	2.07	2.07	–	–
L5×5×5⁄16	11.9	2.99	45	–	3.46	3.46	1.55	1.74	1.74	–	–
L5×3½×¾	16.2	3.25	24.89	13.9	7.06	5.05	1.99	1.92	4.04	10.4	10300
L5×3½×⅝	14.1	2.77	25.26	12.4	6.01	4.33	1.75	1.62	3.34	12.6	6020
L5×3½×½	11.8	2.28	25.60	10.7	4.92	3.56	1.49	1.32	2.67	15.9	3120
L5×3½×⅜	9.19	1.77	25.90	8.57	3.78	2.75	1.2	1.01	2.02	21.4	1330
L5×3½×5⁄16	7.82	1.5	26.05	7.39	3.19	2.33	1.03	0.85	1.69	25.8	775
L5×3½×¼	6.39	1.22	26.18	6.12	2.58	1.89	0.861	0.689	1.36	32.6	399
L5×3×½	10.5	1.57	19.64	7.49	4.82	3.24	1.22	0.975	2.53	16.8	2360
L5×3×7⁄16	9.35	1.4	19.84	6.78	4.27	2.88	1.1	0.862	2.22	19.4	1590
L5×3×⅜	8.19	1.22	20.02	6.02	3.7	2.5	0.983	0.747	1.9	22.8	1010
L5×3×5⁄16	6.97	1.04	20.19	5.19	3.12	2.11	0.854	0.631	1.59	27.6	587
L5×3×¼	5.7	0.851	20.36	4.3	2.53	1.72	0.714	0.512	1.28	34.8	302
L4×4×¾	12	3.29	45	–	4.70	4.70	1.83	2.54	2.54	–	–
L4×4×⅝	10.5	2.80	45	–	4.04	4.04	1.61	2.13	2.13	–	–
L4×4×½	8.83	2.29	45	–	3.33	3.33	1.37	1.72	1.72	–	–
L4×4×7⁄16	7.91	2.04	45	–	2.96	2.96	1.24	1.52	1.52	–	–
L4×4×⅜	6.94	1.77	45	–	2.58	2.58	1.10	1.31	1.31	–	–
L4×4×5⁄16	5.93	1.50	45	–	2.18	2.18	0.953	1.10	1.10	–	–
L4×4×¼	4.85	1.22	45	–	1.77	1.77	0.793	0.893	0.893	–	–

* Refer to Figure 1c for applicable geometry

Table 1. Section Moduli and Lateral-Torsional Constants of Angle Shapes* (cont'd.)											
Angle Shape	I_w (in.^{4})	I_z (in.^{4})	α (deg.)	S_{w1} (in.^{3})	S_{w2} (in.^{3})	S_{w3} (in.^{3})	S_{z1} (in.^{3})	S_{z2} (in.^{3})	S_{z3} (in.^{3})	L_w (in.)	M_{w0} (kip-in.)
L4×3½×½	7.29	1.82	36.87	18.2	3.17	2.75	1.18	1.30	1.74	5.49	7530
L4×3½×⅜	5.75	1.41	37.05	14.9	2.45	2.14	0.948	0.995	1.32	7.38	3230
L4×3½×5⁄16	4.91	1.20	37.13	12.9	2.07	1.81	0.821	0.838	1.11	8.90	1880
L4×3½×¼	4.03	0.976	37.21	10.8	1.69	1.47	0.685	0.679	0.893	11.2	973
L4×3×⅝	7.29	1.62	28.09	9.12	3.77	2.82	1.14	1.17	2.17	7.31	7110
L4×3×½	6.14	1.33	28.49	7.96	3.1	2.34	0.976	0.951	1.73	9.20	3690
L4×3×⅜	4.85	1.03	28.84	6.51	2.39	1.82	0.79	0.728	1.3	12.4	1580
L4×3×5⁄16	4.15	0.876	29.01	5.66	2.02	1.54	0.687	0.614	1.09	15.0	923
L4×3×¼	3.41	0.716	29.16	4.73	1.64	1.26	0.575	0.499	0.88	18.9	477
L3½×3½×½	5.76	1.51	45	–	2.50	2.50	1.01	1.31	1.31	–	–
L3½×3½×7⁄16	5.17	1.35	45	–	2.23	2.23	0.919	1.15	1.15	–	–
L3½×3½×⅜	4.56	1.17	45	–	1.95	1.95	0.818	0.998	0.998	–	–
L3½×3½×5⁄16	3.9	0.995	45	–	1.65	1.65	0.71	0.84	0.84	–	–
L3½×3½×¼	3.21	0.812	45	–	1.34	1.34	0.593	0.679	0.679	–	–
L3½×3×½	4.62	1.16	35.54	11.4	2.38	2.01	0.847	0.947	1.33	4.70	6490
L3½×3×7⁄16	4.17	1.03	35.67	10.4	2.11	1.8	0.769	0.836	1.16	5.38	4390
L3½×3×⅜	3.68	0.896	35.79	9.4	1.84	1.57	0.686	0.724	1.00	6.31	2790
L3½×3×5⁄16	3.15	0.761	35.90	8.23	1.56	1.34	0.597	0.61	0.842	7.61	1630
L3½×3×¼	2.6	0.622	36.01	6.91	1.27	1.09	0.500	0.495	0.680	9.57	843
L3½×2½×½	3.82	0.784	25.92	4.93	2.32	1.69	0.676	0.655	1.32	7.50	3210
L3½×2½×⅜	3.04	0.609	26.40	4.08	1.80	1.32	0.55	0.501	0.986	10.1	1380
L3½×2½×5⁄16	2.61	0.519	26.62	3.57	1.53	1.12	0.481	0.423	0.825	12.2	803
L3½×2½×¼	2.15	0.425	26.83	3.00	1.24	0.916	0.405	0.344	0.664	15.4	415
L3×3×½	3.49	0.938	45	–	1.80	1.8	0.712	0.957	0.957	–	–
L3×3×7⁄16	3.16	0.833	45	–	1.61	1.61	0.647	0.842	0.842	–	–
L3×3×⅜	2.79	0.726	45	–	1.40	1.40	0.579	0.727	0.727	–	–
L3×3×5⁄16	2.40	0.617	45	–	1.19	1.19	0.504	0.612	0.612	–	–
L3×3×¼	1.98	0.504	45	–	0.976	0.976	0.423	0.495	0.495	–	–
L3×3×3⁄16	1.54	0.388	45	–	0.747	0.747	0.334	0.377	0.377	–	–
L3×2½×½	2.71	0.677	33.69	6.51	1.70	1.40	0.574	0.651	0.977	3.89	5470
L3×2½×7⁄16	2.45	0.601	33.88	6.04	1.52	1.25	0.523	0.574	0.854	4.46	3700
L3×2½×⅜	2.17	0.525	34.06	5.48	1.32	1.10	0.468	0.497	0.733	5.23	2360
L3×2½×5⁄16	1.87	0.446	34.22	4.84	1.13	0.935	0.409	0.419	0.614	6.31	1380
L3×2½×¼	1.55	0.366	34.37	4.1	0.919	0.765	0.345	0.34	0.496	7.94	714
L3×2½×3⁄16	1.20	0.281	34.52	3.25	0.704	0.587	0.274	0.26	0.376	10.7	305
L3×2×½	2.18	0.413	22.50	2.8	1.66	1.15	0.433	0.417	0.971	5.78	2730

* Refer to Figure 1c for applicable geometry

Table 1. Section Moduli and Lateral-Torsional Constants of Angle Shapes* (cont'd.)											
Angle Shape	I_w (in.^{4})	I_z (in.^{4})	α (deg.)	S_{w1} (in.^{3})	S_{w2} (in.^{3})	S_{w3} (in.^{3})	S_{z1} (in.^{3})	S_{z2} (in.^{3})	S_{z3} (in.^{3})	L_w (in.)	M_{w0} (kip-in.)
L3×2×3/8	1.75	0.32	23.18	2.36	1.29	0.904	0.354	0.318	0.713	7.80	1170
L3×2×5/16	1.51	0.273	23.49	2.08	1.10	0.771	0.311	0.268	0.593	9.44	685
L3×2×1/4	1.25	0.225	23.77	1.77	0.895	0.632	0.264	0.218	0.476	11.9	354
L3×2×3/16	0.975	0.174	24.03	1.40	0.685	0.486	0.211	0.167	0.36	16.1	151
L2½×2½×½	1.92	0.533	45	–	1.21	1.21	0.468	0.662	0.662	–	–
L2½×2½×3/8	1.56	0.412	45	–	0.952	0.952	0.382	0.5	0.5	–	–
L2½×2½×5/16	1.35	0.35	45	–	0.813	0.813	0.335	0.421	0.421	–	–
L2½×2½×1/4	1.12	0.287	45	–	0.667	0.667	0.283	0.341	0.341	–	–
L2½×2½×3/16	0.872	0.221	45	–	0.513	0.513	0.225	0.259	0.259	–	–
L2½×2×3/8	1.15	0.273	31.56	2.85	0.893	0.708	0.294	0.314	0.509	4.14	1930
L2½×2×5/16	1.00	0.233	31.81	2.55	0.762	0.607	0.258	0.264	0.424	4.99	1130
L2½×2×1/4	0.835	0.191	32.05	2.18	0.624	0.500	0.219	0.215	0.341	6.28	587
L2½×2×3/16	0.652	0.148	32.26	1.75	0.48	0.385	0.175	0.164	0.258	8.46	251
L2×2×3/8	0.752	0.206	45	–	0.587	0.587	0.229	0.318	0.318	–	–
L2×2×5/16	0.658	0.175	45	–	0.504	0.504	0.201	0.266	0.266	–	–
L2×2×1/4	0.552	0.143	45	–	0.416	0.416	0.171	0.215	0.215	–	–
L2×2×3/16	0.434	0.111	45	–	0.322	0.322	0.138	0.164	0.164	–	–
L2×2×1/8	0.303	0.0766	45	–	0.221	0.221	0.0991	0.112	0.112	–	-

* Refer to Figure 1c for applicable geometry

Substitution of Equation 5 into Equation 6 yields:

$$\frac{M_n}{M_y} = 1.92 - 0.729\frac{\gamma}{\sqrt{C_b}}\sqrt{1+\sqrt{1+0.78\varpi^2}} \le 1.5 \qquad (7)$$

For ϖ ranging of 0.2 to 7.0, the square root in Equation 7 is very close to a straight line, within ±2.0%:

$$\sqrt{1+\sqrt{1+0.78\varpi^2}} \cong 0.20\ \varpi + 1.35 \qquad (8)$$

Accordingly, the combination of Equations F10-3 and F10-4a of the AISC *Specification* may be expressed with the formula:

$$\frac{M_n}{M_y} \approx 1.92 - \left(1.0 + 0.15\varpi\right)\frac{\gamma}{\sqrt{C_b}} \le 1.5 \qquad (9)$$

For practical spans with the toes in compression, the results of Equation 9 compared to those of F10-3 and F10-4a are always within 2%.

In the case of maximum tension at the toes, Equation 5 becomes

$$\frac{M_y}{M_e} \approx 0.388\frac{\gamma^2}{C_b}\left(\sqrt{1+0.78\varpi^2}-1\right) = 0.303\ \frac{\gamma^2}{C_b}\ \frac{\varpi^2}{+\sqrt{+0.78\varpi^2}} \qquad (10)$$

This leads to

$$\frac{M_n}{M_y} \approx 1.92 - 0.644\frac{\gamma}{\sqrt{C_b}}\frac{\varpi}{\sqrt{1+\sqrt{1+0.78\varpi^2}}} \le 1.5 \qquad (11)$$

Making use of Equation 8 to replace the radical in Equation 11, the final result for tension at the toes is then, within 2% compared to F10-3 and F10-4a,

$$\frac{M_n}{M_y} \approx 1.92 - \frac{\varpi}{0.31\ \varpi + 2.1}\frac{\gamma}{\sqrt{C_b}} \le 1.5 \qquad (12)$$

Of all hot-rolled equal-leg angles, the most slender shape is the L6×6×5/16 with b/t = 19.2, or γ = 0.676 (F_y = 36 ksi). For M_e/M_y to reach the value of 1.0 with the toes in compression, ϖ must be at least 5, and the beam should have an unrealistic span of nearly 50 ft. The span would still be at least 30 ft for F_y = 50 ksi. As mentioned earlier, with hot-rolled equal-leg angles, Equation F10-2 never governs. The calculations are then fairly simple. If the tip of the outstanding leg is in compression, consider these factors corresponding to the three limit states:

Yielding $k_1 = 1.5$ (13a)

Lateral-torsional buckling $k_2 = 1.92 - \left(0.15\varpi + 1.0\right)\dfrac{\gamma}{\sqrt{C_b}}$ (13b)

Local buckling $k_3 = 2\,43 - 1\,72\gamma$ (13c)

Let k_m equal the smallest of the three; the design bending strength is then $\phi M_n = \phi k_m F_y(0.80S_x)$. To avoid having to look up the value of S_x, the following approximation will be found adequate

$$S_x \approx 0.276t\left(b - 0.43t\right)^2 \tag{14}$$

If the tip of the outstanding leg is in tension, local buckling does not occur, and the factor f_2 is equal to the right-hand side of Equation 12. Single-angle members are not very efficient beams, and, in many cases, the order of magnitude of the deflection should be checked. Without lateral support, the vertical deflection may be computed with an equivalent moment of inertia $I_{eq} \approx 0.65I_x \approx 0.075b^3t$; in most cases, this deflection should not exceed $L/300$.

LATERAL-TORSIONAL BUCKLING ABOUT PRINCIPAL AXES (EQUAL- AND UNEQUAL-LEG ANGLES)

The general method using the principal axes of the angle is based on Equation F10-6 of the AISC *Specification*

$$M_e = \frac{4.9EC_bI_z}{L^2}\left(\sqrt{\beta_w^2 + 0.052\left(\frac{Lt}{r_z}\right)^2} \pm \beta_w\right) \tag{15}$$

This formula is the specialized result of a bifurcation analysis of the elastic lateral-torsional stability of prismatic members (Timoshenko and Gere, 1961). Using the symbols of the AISC *Specification* and adding the moment modification factor C_b, the elastic buckling moment of an angle is

$$M_e = C_b\left(\sqrt{\left(\frac{P_{ez}\beta_w}{2}\right)^2 + GJP_z} \pm \frac{P_{ez}\beta_w}{2}\right) \tag{16}$$

P_{ez} is the Euler buckling load about the minor axis of inertia

$$P_{ez} = \frac{\pi^2 EI}{L^2} = \frac{\pi^2 EAr_z^2}{L^2} \tag{17}$$

GJ is the torsional rigidity of the angle

$$GJ = \frac{1}{3}GAt^2 = \frac{1}{3}Gt^3(d + b - t) \tag{18}$$

For unequal leg angles, β_w is not zero, and Equation 15 may be recast in the form

$$M_e = C_b\frac{P_z\beta_w}{2}\left(\sqrt{1 + \frac{4GJ}{P_z\beta_w^2}} \pm 1\right) \tag{19}$$

It is convenient to introduce a parameter u, such that

$$u^2 = \left(\frac{L}{\ell_w}\right)^2 = \frac{4GJ}{P_z\beta_w^2} = 0.0520\left(\frac{Lt}{\beta_w r_z}\right)^2 \tag{20}$$

The length ℓ_w is a characteristic of the section, listed in Table 1:

$$\ell_w = 4.385\frac{\beta_w r_z}{t} \tag{21}$$

From Equation 20, it is easily seen that

$$\frac{P_z\beta_w}{2} = \frac{2GJ}{\beta_w u^2} \tag{22}$$

Equation 19 may now be written

$$M_e = C_b\frac{2GJ}{\beta_w}\left[\frac{\left(\sqrt{1+u^2}\right) \pm 1}{u^2}\right] = \frac{C_bM_{w0}}{\left(\sqrt{1+u^2}\right) \pm 1} \tag{23}$$

Note that the quantity $M_{w0} = 2GJ/\beta_w$ has the dimensions of a moment and is a characteristic of the section, also listed in Table 1.

In the expression

$$M_e = C_b\,M_{w0}\Big/\left(\sqrt{1 + \left(\frac{L}{\ell_w}\right)^2} \pm 1\right) \tag{24}$$

the plus sign applies if the long leg is anywhere in compression, and the minus sign otherwise.

For practical spans with hot-rolled angles, the ratio M_y/M_e is smaller than 1.0, and buckling, if it occurs, occurs in the inelastic range. In other words, Equation F10-3 of the AISC *Specification* (given as Equation 6 previously) governs. Therefore, Equation F10-3 may be written

$$\frac{M_{nw(i)}}{M_{y(i)}} = 1.92 - 1.17\sqrt{\frac{F_y\,S_{w(i)}}{M_e}} \le 1.5 \tag{25}$$

Table 2. Geometric Axis Bending Strength ϕM_{nx} Using Principal and Geometric Axes					
Angle Shape	L (ft)	Design Bending Strength ϕM_{nx}			
		Principal Axes		Geometric Axes	
		C	T	C	T
L8×8×½	6	315	321	284	325
	8	309	315	281	325
	10	305	311	278	325
	12	300	305	275	325
	16	290	295	268	325
	20	280	285	260	325
L6×6×5/16	4	97.5	114	91.7	115
	6	97.5	110	90.7	115
	8	96.2	107	89.4	115
	10	93.4	104	87.9	115
	12	91.4	101	86.2	115
	16	86.8	95.5	82.8	113
L4×4×¼	4	38.8	39.6	35.3	40.8
	5	37.9	38.7	34.9	40.8
	6	37.6	38.2	34.5	40.8
	8	36.0	36.7	33.6	40.8
	10	34.8	35.5	32.6	40.8
	12	33.8	34.2	31.7	39.6
Horizontal moments M_x are in kip-in., with C_b =1.0 and F_y = 36 ksi. "C" denotes toe (Point 3) in compression, "T" toe in tension.					

Because the parameter u varies over a much larger range than ϖ, a linear approximation similar to Equation 8 is not possible. The nominal bending strength M_{nw} must be computed at the three points of consideration i = 1, 2, 3. For equal-leg angles, the length β_w is nil, and the elastic buckling moment is

$$M_e = \sqrt{GJP_z} \approx 0.46 C_b E \frac{b^2 t^2}{L} \qquad (26)$$

This approximation is the formula included in the AISC *Specification*. Which is preferable, the geometric or the principal axis method. Comparative results are listed in Table 2, which shows the design horizontal moment, ϕM_{nx}, computed with both methods. In that comparison, the three limit states are included in accordance with the AISC *Specification*. The principal axis method appears more conservative for the toe in tension, the geometric axis method for the toe in compression.

COMBINED FORCES AND DUE REGARD TO SIGNS

Lutz (1996) and Sakla (2001) have shown the importance of attaching the proper signs to the several terms of the interaction equations. However, a substantial change from the previous specification for single angles—which allowed the use of Equations H1-1a and H1-1b—is that the current AISC *Specification* (AISC, 2005) restricts their use to "…singly symmetric members…that are constrained to bend about a *geometric axis* (*x* and/or *y*)…". A strict interpretation of the AISC *Specification* is that the governing clause is Section H2, and the applicable interaction equation is H2-1, reproduced here:

$$\left| \frac{f_a}{F_a} + \frac{f_{bw}}{F_{bw}} + \frac{f_{bz}}{F_{bz}} \right| \le 1.0$$

The AISC *Specification* also states that

$$F_a = \phi F_{cr} \qquad F_{b_w} = \phi M_{nw} / S_w \qquad F_{bz} = \phi M_{nz} / S_z \qquad (27)$$

Section H2 adds: "Use the section modulus for the specific location in the cross-section and consider the sign of the stress." Accordingly, H2-1 may be written

$$\left| \frac{P_r}{\phi P_n} \pm \frac{M_{rw}}{\phi M_{nw}} \pm \frac{M_{rz}}{\phi M_{nz}} \right| \le 1.0 \qquad (28)$$

It is always permissible, but often overly conservative, to replace the absolute value in Equation 28 with the sum of the absolute values of its terms. It is usually advantageous to take the sense of the stress into account. The systematic use of a sign convention is helpful; the author uses that of Figure 3 (although it is not the only valid one by any means).

If the toe of the short leg is always taken as Point 2, positive moments M_w and M_z cause Point 2 to be in compression. A positive moment M_x gives $M_w > 0$ and $M_z < 0$ as shown on Figure 4. A positive moment M_y gives both $M_w > 0$ and $M_z > 0$. The combinations for the points of consideration 1, 2 and 3 are then

$$\begin{aligned} \left| \frac{P_r}{\phi P_n} + \frac{M_{rw}}{\phi M_{nw}[1]} - \frac{M_{rz}}{\phi M_{nz}[1]} \right| &\le 1.0 \\ \left| \frac{P_r}{\phi P_n} + \frac{M_{rw}}{\phi M_{nw}[2]} + \frac{M_{rz}}{\phi M_{nz}[2]} \right| &\le 1.0 \\ \left| \frac{P_r}{\phi P_n} - \frac{M_{rw}}{\phi M_{nw}[3]} + \frac{M_{rz}}{\phi M_{nz}[3]} \right| &\le 1.0 \end{aligned} \qquad (29)$$

SINGLE-ANGLE COMPRESSION MEMBERS

Section E5 of the AISC *Specification*, entitled "Single Angle Compression Members" introduces the notion of an effective slenderness ratio *KL/r* to account for the effects of eccentricity and end restraints inherent to single angles used as web members. Lutz (2006) provides the background for this approach, which has been common practice in steel transmission tower design (ASCE, 1988, 1992; ECCS, 1976).

The Appendix recasts Equations E5-1 to E5-4 in what is believed to be a slightly clearer form. Note that the validity of Section E5 is restricted to angles with a leg length ratio $\rho = b_l/b_s < 1.7$, thereby excluding the sizes L8×4, L7×4 and L6×3½, which must be handled as eccentrically loaded columns.

Normally, connecting through the long leg is less efficient than through the short leg. Except for $L/r_y < 20$, the long-leg connection has a larger *KL/r* ratio, hence less strength. The reverse situation for $L/r_y < 20$ is due to the length-independent terms $4(\rho^2 - 1)$ or $6(\rho^2 - 1)$. However, as this occurs in the inelastic range of the column curve, the difference in design strengths is insignificant. For instance, a 10-in. long L3×2×¼ strut (an unusually stocky web member) has a ratio $L/r_y = 17.4$. Attached through the long leg, $KL/r = 73.9$ and $\phi P_n = 28.9$ kips; connected through the short leg, $KL/r = 75.9$ and $\phi P_n = 28.4$ kips, a very small difference indeed. For members of usual proportions and barring other considerations, web members connected to the chord or gusset through the short leg are more efficient.

To help the designer find the minimum-weight equal-leg angle, Tables 3 and 4 may be useful. They are limited to equal-leg shapes; the former applies to box trusses, the latter to planar trusses. The tables list the least-weight sections for member lengths ranging from 5 to 16 ft and required axial strengths from 10 to 50 kips. Also listed are the unit weight and the design axial strength $P_c = \phi P_n$. The shaded cells in the tables cover combinations of lengths and axial forces that are, in the writer's experience, unlikely to occur in practice.

The tables do not address the question of whether equal-leg web members are more efficient than unequal-leg angles connected through the short leg, a question without a clear answer. In general, an equal-leg angle will be stronger than the unequal-leg angle of the same weight, but not always. In most cases, the differences are small enough to make it reasonable to standardize on only a few equal-leg sizes for a given job.

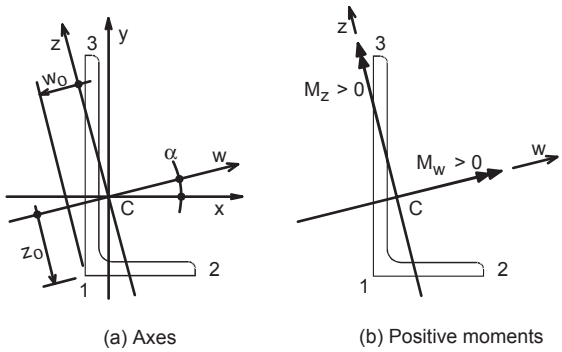

Fig. 3. System of principal axes.

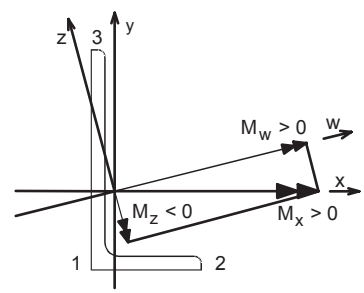

Fig. 4. Bending about geometric axis x-x.

Table 3. Single Equal-Leg Angles as Web Members of Box or Space Trusses: Least-Weight Sections								
Length L, ft		Required Axial Strength P_r, kips (LRFD)						
		10	15	20	25	30	40	50
5	Size	L2½×2½×3/16	L3×3×3/16	L3×3×¼	L3½×3½×¼	L3½×3½×¼	L4×4×5/16	L4×4×⅜
	lb/ft	3.07	3.71	4.89	5.74	5.74	8.17	9.72
	P_c	13.3	17.8	24.2	30.5	30.5	46.6	55.4
6	Size	L2½×2½×3/16	L3×3×3/16	L3×3×¼	L3½×3½×¼	L4×4×¼	L4×4×5/16	L4×4×⅜
	lb/ft	3.07	3.71	4.89	5.74	6.59	8.17	9.72
	P_c	10.8	15.8	21.2	27.7	33.4	42.9	50.9
7	Size	L3×3×3/16	L3×3×¼	L3½×3½×¼	L4×4×¼	L4×4×¼	L4×4×⅜	L5×5×5/16
	lb/ft	3.71	4.89	5.74	6.59	6.59	9.72	10.3
	P_c	13.5	17.7	24.8	30.8	30.8	46.5	53.8
8	Size	L3×3×3/16	L3½×3½×¼	L3½×3½×¼	L4×4×¼	L4×4×5/16	L4×4×⅜	L5×5×5/16
	lb/ft	3.71	5.74	5.74	6.59	8.17	9.72	10.3
	P_c	11.4	21.5	21.5	28.1	35.4	41.9	50.5
10	Size	L3×3×¼	L3½×3½×¼	L4×4×¼	L4×4×5/16	L4×4×⅜	L5×5×5/16	L5×5×⅜
	lb/ft	4.89	5.74	6.59	8.17	9.72	10.3	12.3
	P_c	10.7	15.9	22.1	27.1	31.9	44.0	53.1
12	Size	L3½×3½×¼	L4×4×¼	L4×4×5/16	L5×5×5/16	L5×5×5/16	L5×5×⅜	L6×6×5/16
	lb/ft	5.74	6.59	8.17	10.3	10.3	12.3	12.4
	P_c	12.2	17.1	21.0	36.3	36.3	43.1	51.6
14	Size	L4×4×¼	L4×4×5/16	L5×5×5/16	L5×5×5/16	L5×5×⅜	L6×6×5/16	L6×6×⅜
	lb/ft	6.59	8.17	10.3	10.3	12.3	12.4	14.8
	P_c	13.6	16.7	29.5	29.5	34.9	44.8	54.1
16	Size	L4×4×¼	L5×5×5/16	L5×5×5/16	L5×5×⅜	L6×6×5/16	L6×6×⅜	L6×6×7/16
	lb/ft	6.59	10.3	10.3	12.3	12.4	14.8	17.2
	P_c	11.1	24.3	24.3	28.8	38.3	45.5	52.4

Notes: 1. $P_c = \phi P_n$ is the design compressive axial strength (LRFD), kips, using ASTM A36 steel (F_y = 36 ksi).
2. Web members must be welded or bolted (two bolts minimum) on same side of chord or gusset.

The AISC *Specification* is silent on the subject of single-angle truss chords or legs. Both the ASCE Manual (1988) and the ASCE Standard ANSI/ASCE 10-90 specify that single-angle tower leg members (i.e., chords braced in both directions) may be designed using $KL/r = L/r_z$, where L is the system length and r_z the minor radius of inertia. In addition, both documents limit the ratio L/r_z to a maximum value of 150. This recommendation is followed in Table 5, which lists least-weight equal-leg angles for chord members.

BEHAVIOR OF AXIALLY LOADED SINGLE ANGLES

The behavior predicted by Chapter H for unsymmetrical angles is in contradiction with what Section E5 leads one to expect. According to Section E5, angles with practical slenderness ratios are substantially stronger if they are connected through the short leg. The beam-column approach of Chapter H leads to the opposite conclusion (Sakla, 2001): from a maximum if the load is applied at the centroid, the axial strength would fall off rapidly away from the centroid. Dr. Lutz's comments (2006) show how difficult it is to reconcile the experimental evidence embodied in Section E5 with the beam-column approach of Chapter H. Section E5 is based on an experimental program intended to validate a simpler approach, similar to that in the ASCE Standard (Mengelkoch and Yura, 2002). More recently, finite element models have been used to further support Section E5 (Earls and Keelor, 2007).

To gain some insight into the behavior of an axially loaded single angle, consider such an angle hinged at both ends.

Table 4. Single Equal-Leg Angles as Web Members of Planar Trusses: Least-Weight Sections								
Length L, ft		Required Axial Strength P_r, kips (LRFD)						
		10	15	20	25	30	40	50
5	Size	L2½×2½×3⁄16	L3×3×3⁄16	L3×3×¼	L3½×3½×¼	L4×4×¼	L4×4×5⁄16	L5×5×5⁄16
	lb/ft	3.07	3.71	4.89	5.74	6.59	8.17	10.3
	P_c	12.0	16.1	21.7	27.5	32.7	42.0	55.0
6	Size	L3×3×3⁄16	L3×3×¼	L3½×3½×¼	L4×4×¼	L4×4×¼	L4×4×3⁄8	L5×5×5⁄16
	lb/ft	3.71	4.89	5.74	6.59	6.59	9.72	10.3
	P_c	14.4	19.1	24.9	30.3	30.3	45.8	51.9
7	Size	L3×3×3⁄16	L3×3×¼	L3½×3½×¼	L4×4×¼	L4×4×5⁄16	L4×4×3⁄8	L5×5×3⁄8
	lb/ft	3.71	4.89	5.74	6.59	8.17	9.72	12.3
	P_c	11.9	15.5	22.4	27.9	35.2	41.8	59.7
8	Size	L3×3×¼	L3½×3½×¼	L4×4×¼	L4×4×¼	L4×4×5⁄16	L5×5×5⁄16	L5×5×3⁄8
	lb/ft	4.89	5.74	6.59	6.59	8.17	10.3	12.3
	P_c	12.5	18.9	25.6	25.6	32.0	45.8	55.7
10	Size	L3½×3½×¼	L4×4×¼	L4×4×5⁄16	L4×4×3⁄8	L5×5×5⁄16	L5×5×5⁄16	L6×6×5⁄16
	lb/ft	5.74	6.59	8.17	9.72	10.3	10.3	12.4
	P_c	13.3	19.0	23.3	27.4	40.0	40.0	52.4
12	Size	L4×4×¼	L4×4×5⁄16	L4×4×3⁄8	L5×5×5⁄16	L5×5×5⁄16	L6×6×5⁄16	L6×6×3⁄8
	lb/ft	6.59	8.17	9.72	10.3	10.3	12.4	14.8
	P_c	14.2	17.4	20.4	31.7	31.7	47.3	57.6
14	Size	L5×5×5⁄16	L5×5×5⁄16	L5×5×5⁄16	L5×5×3⁄8	L6×6×5⁄16	L6×6×5⁄16	L6×6×7⁄16
	lb/ft	10.3	10.3	10.3	12.3	12.4	12.4	17.2
	P_c	24.8	24.8	24.8	29.3	40.1	40.1	54.9
16	Size	L5×5×5⁄16	L5×5×5⁄16	L5×5×3⁄8	L6×6×5⁄16	L6×6×5⁄16	L6×6×7⁄16	L6×6×½
	lb/ft	10.3	10.3	12.3	12.4	12.4	17.2	19.6
	P_c	19.9	19.9	23.5	32.6	32.6	44.4	50.1

Notes: 1. $P_c = \phi P_n$ is the design compressive axial strength (LRFD), kips, using ASTM A36 steel (F_y = 36 ksi).
2. Web members must be welded or bolted (two bolts minimum) on same side of chord or gusset.

The elastic bifurcation buckling load P may be found from a general equation developed in Timoshenko and Gere (1961), specialized for axially loaded angles by dropping the bending moments M_1 and M_2 and setting $C_w = 0$:

$$f(P) = \begin{vmatrix} P_{ez} - P & 0 & P(e_z - z_0) \\ 0 & P_{ew} - P & -P(e_w - w_0) \\ P(e_z - z_0) & -P(e_w - w_0) & GJ \quad -Ps_1 \end{vmatrix} = 0 \quad (30)$$

In this equation, w_0 and z_0 are the coordinates of the shear center, and e_w and e_z are the eccentricities of the point of application, relative to the centroid. The other symbols are:

$$P_{ew} = \frac{\pi^2 EI_w}{L^2} \qquad P_{ez} = \frac{\pi^2 EI_z}{L^2}$$
$$s_1 = \beta_w e_z + \beta_z e_w + r_w^2 + r_z^2 + w_0^2 + z_0^2$$
$$\beta_w = \frac{1}{I_w}\int_A z(w^2 + z^2)\,dA - 2z_0 \qquad (31)$$
$$\beta_z = \frac{1}{I_z}\int_A w(w^2 + z^2)\,dA - 2w_0$$

Care must be taken to apply the proper signs to the torsional parameters β_w and β_z and to the coordinates w_0 and z_0 of the shear center. For instance with the sign conventions of Figure 3, β_w and β_z are positive, w_0 and z_0 negative. Equation 30

Table 5. Single Equal-Leg Angles as Chord Members of Box Trusses: Least-Weight Sections								
Length L, ft		Required Axial Strength P_r, kips (LRFD)						
		20	25	30	40	50	65	80
4	Size	L3×3×3/16	L3×3×¼	L3×3×¼	L3½×3/½×¼	L3½×3/½×5/16	L4×4×⅜	L3½×3/½×½
	lb/ft	3.71	4.89	4.89	5.74	7.11	9.72	11.0
	P_c	23.6	33.0	33.0	41.4	52.5	76.2	81.2
5	Size	L3×3×¼	L3×3×¼	L3½×3½×¼	L4×4×¼	L4×4×5/16	L4×4×⅜	L5×5×⅜
	lb/ft	4.89	4.89	5.74	6.59	8.17	9.72	12.3
	P_c	27.1	27.1	36.1	43.5	57.4	68.3	95.0
6	Size	L3×3×¼	L3½×3½×¼	L3½×3½×¼	L4×4×5/16	L4×4×5/16	L5×5×5/16	L5×5×⅜
	lb/ft	4.89	5.74	5.74	8.17	8.17	10.3	12.3
	P_c	21.4	30.5	30.5	50.2	50.2	69.5	87.4
7	Size	L3½×3½×¼	L3½×3½×¼	L4×4×¼	L4×4×5/16	L4×4×⅜	L5×5×⅜	L5×5×7/16
	lb/ft	5.74	5.74	6.59 lb/ft	8.17	9.72	12.3	14.2
	P_c	25.0	25.0	33.5	42.9	50.9	79.2	92.5
8	Size	L4×4×¼	L4×4×¼	L4×4×5/16	L4×4×⅜	L5×5×5/16	L5×5×⅜	L5×5×7/16
	lb/ft	6.59	6.59	8.17	9.72	10.3	12.3	14.2
	P_c	28.4	28.4	35.8	42.4	57.1	70.6	82.3
10	Size	L5×5×5/16	L5×5×5/16	L5×5×5/16	L5×5×5/16	L5×5×⅜	L6×6×⅜	L6×6×7/16
	lb/ft	10.3	10.3	10.3	10.3	12.3	14.8	17.2
	P_c	44.4	44.4	44.4	44.4	53.7	79.2	94.6
12	Size	L5×5×5/16	L5×5×5/16	L5×5×5/16	L6×6×5/16	L6×6×5/16	L6×6×7/16	L6×6×½
	lb/ft	10.3	10.3	10.3	12.4	12.4	17.2	19.6
	P_c	32.6	32.6	32.6	52.1	52.1	75.2	85.6
14	Size	L6×6×5/16	L6×6×5/16	L6×6×5/16	L6×6×5/16	L6×6×7/16	L6×6×9/16	L8×8×½
	lb/ft	12.4	12.4	12.4	12.4	17.2	21.9	26.4
	P_c	41.5	41.5	41.5	41.5	57.2	71.9	134

Notes: 1. $P_c = \phi P_n$ is the design compressive axial strength (LRFD), kips, using A36 steel (F_y = 36 ksi).
2. KL/rz is limited to 150.

is a cubic equation in P, whose smallest positive root is the critical or elastic buckling load P. Knowing that $0 < P \le P_{ez}$, the equation may be solved by a numerical method such as the Birge-Vieta iteration (Hildebrand, 1987).

If the ends of the angle are fully restrained, Equation 30 still applies, except that P_{ew} and P_{ez} are multiplied by 4. Yu (1985) lists similar equations that include certain factors reflecting different end restraints. All these equations have the same form, which shows that while the quantitative results will be somewhere between the two extremes of full restrained or hinged ends, the qualitative behavior will remain the same. Therefore, Equation 30 provides a good behavioral model for an axially loaded single-angle member.

If $e_z = z_0$, Equation 30 breaks down into two equations

$$P = P_{ez} \tag{32a}$$

$$(P_{ew} - P)(GJ - Ps_1) - P^2(e_w - w_0)^2 = 0 \tag{32b}$$

The condition $e_z = z_0$ means that the load is applied on a line $S - w'$ issued from the shear center S parallel to w-w as shown on Figure 5. Furthermore, if the coordinate e_w is not larger that a certain value e_{w1}, the critical load is constant and equal to P_{ez}. If the load is applied to the right of point M, then Equation 32b has a root smaller than P_{ez}, and that root is the critical load. Since an equal-leg angle is singly symmetric, line $S - w'$ is of course the principal axis w-w. Note, however,

that the sign of the coordinate e_{w1} depends on several parameters, in particular the length L of the member. For instance, for a L5×5×5/16 angle, e_{w1} = –0.54 in. for L = 60 in., +0.03 in. for L = 84 in., and +0.39 in. for L = 96 in. For shorter spans and thinner angles, the critical load at the centroid may be considerably less than that at the shear center.

The general case of an axially loaded unequal-leg angle (or of an unsymmetrical open shape in general) does not seem to have been investigated to any extent. Usually, the discussion is limited to the fact that if the load is applied at the shear center, Equations 32 replace Equation 30, and the buckling modes are uncoupled (Timoshenko and Gere, 1961). Since the centroid of a unequal-leg angle is not on line *S-w'*, applying the axial thrust at the centroid results in a critical load always less than at the shear center, P_{ez}. For instance, a 96-in.-long L6×4×3/8 has an elastic buckling load $P = P_{ez}$ = 86.3 kips if the thrust is applied at the shear center, and $P = 0.90P_{ez}$ = 77.1 kips if it is applied at the centroid.

The behavior of eccentrically loaded angles predicted by Section E5 is qualitatively confirmed by the results of Equation 30. Examining these results is easier if we use the distances δ_x and δ_y shown on Figure 6. Consider again the 96-in.-long L6×4×3/8. If it is attached through its long leg to a chord or gusset ½ in. thick, it could be assumed that the load is applied in the plane of contact ($\delta_x = 0$) at the middle of the long leg (δ_y = 3 in.). This assumption leads to P = 63.5 kips. If applying the load in the plane of contact might be judged too optimistic, move the axial force to the centerline of the gusset, or δ_x = –0.25 in. away; the critical load becomes P = 63.3 kips, a negligible decrease. On the other hand, if the angle is connected through its short leg so that δ_x = 2 in. and δ_y = 0, the critical load is P = 83.9 kips for δ_y = 0, decreasing to P = 82.9 kips for δ_y = –0.25 in. Since there is no apparent reason why the axial force should be acting at mid-thickness of the chord rather than at mid-thickness of the web member, it seems reasonable to assume that the transfer of force takes place in the plane of contact. In any case, theory confirms that connecting an angle through its short leg is more efficient than attaching it through its long leg.

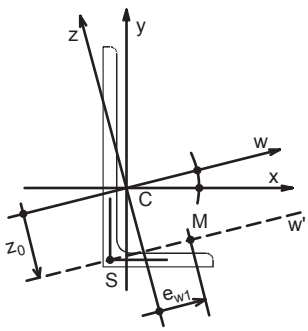

Fig. 5. Shear center S *and line* S-w'.

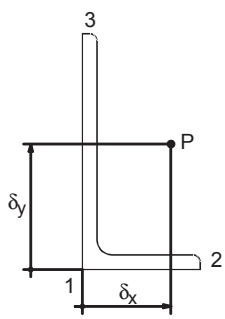

Fig. 6. Point of application of axial load.

Figure 7 presents results obtained by moving the axial load in the plane of contact, that is, along the outside perimeter of the angle. The curve for an L5×5×3/8 is not shown, as it is practically identical to that for an L6×4×3/8 attached through the long leg, shown on the figure. The elastic buckling load for either short- or long-leg connection does not vary much in the vicinity of the shear center, but falls off rather rapidly for equal-leg angles or unequal-leg angles attached through the long leg. From a stability standpoint, a single-angle member, web or chord, is more efficiently loaded at or near its shear center. Flexural yielding considerations may modify this conclusion.

The elastic critical load depends on the thickness t of the angle. In the determinant of Equation 30, the parameter s_1 is nearly independent of t, the Euler loads are roughly proportional to t, while the torsional rigidity GJ increases with the cube of t. Increasing the thickness reduces the twisting tendency of the member, which is translated by flatter curves than those shown on Figure 7. In other words, thicker angles are less sensitive to axial load location; the L5×5×3/8, whose curve is the same as that of the L6×4×3/8 attached through the long leg, has a smaller fall-off than the thinner L5×5×5/16.

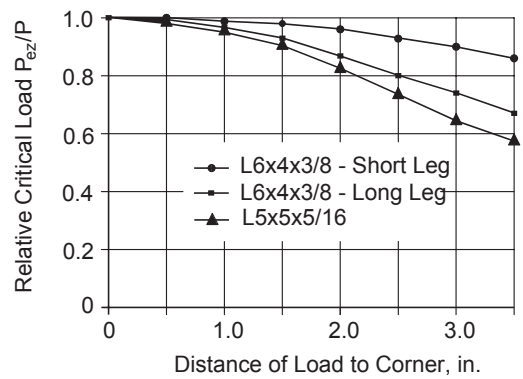

Fig. 7. Relative critical load of 8-ft-long single-angle loaded in plane of contact.

The complete differential equations derived by Timoshenko and Gere (1961) include not only the thrust, P, which may be eccentric, but also two end moments about the principal axes, M_1 and M_2 (M_1 is the buckling moment listed in Equation 15). It is obvious from the very form of these equations that there is a strong interaction between axial force and moments. If there is an axial thrust P, the presence of constant moments has for only effect to increase or decrease the eccentricities e_w and e_z. While it may lead to a safe design, simply adding the effects of the two types of loads as in a beam-column does not seem consistent with the behavior of a single angle.

CONCLUSIONS

Several arguments, not the least being simplicity, are presented to limit the number of critical points or "points of consideration" in the cross- section of a steel angle to three. Table 1 lists the corresponding section moduli.

The several clauses in the AISC *Specification* governing lateral-torsional buckling are examined, and some simplifications are proposed. Calculations summarized in Table 2 show that the geometric and principal axis approaches lead to somewhat different results, but not exceedingly so. Suggestions are made regarding due regard to stress signs recommended by the AISC *Specification*.

Section E5 of the AISC *Specification* is a very welcome simplification for the design of single-angle web members. Tables 3, 4 and 5 are presented to aid the designer in the selection of economical sizes in accordance with the requirements of that Section.

Not only has Section E5 introduced a new approach in to the design of eccentrically loaded single-angle web members, it also shows that connecting such members through the short leg is a more efficient use of material. This, however, is in contradiction with the results of beam-column calculations specified in Sections E3 or E7, according to which connecting an angle through its long leg would indicate a stronger member. A theoretical equation presented by Timoshenko and Gere (1961)is used to examine the qualitative behavior of eccentrically loaded single angles. According to it, the shear center plays a key role in the behavior of a steel angle, and the load transfer from chord to web may be assumed to take place in the plane of contact. The elastic critical load is not too sensitive to the position of the load along the connected leg. Finally, it confirms the experimental evidence that an angle is stronger if it is connected through its short leg.

REFERENCES

AISC (2000), *Load and Resistance Factor Design Specification for Single-Angle Members,* American Institute of Steel Construction, Chicago, IL.

AISC (2005), *Specification for Steel Buildings—ANSI/AISC 360-05,* American Institute of Steel Construction, Chicago, IL.

ASCE (1988), *Manual of Standard Practice No. 52, Guide for Design of Steel Transmission Towers,* 2nd edition, American Society of Civil Engineers, Reston, VA.

ASCE (1992), *Design of Latticed Steel Transmission Structures—ANSI/ASCE 10-90,* American Society of Civil Engineers, Reston, VA.

ECCS (1976), Introductory Report, Sub-Chapter 3.1.5, "Angles" and Sub-Chapter 9.2, "Angles in Lattice Transmission Towers," *Proceedings from the Second International Colloquium on Stability.*

Earls, C.J. and Keelor, D. Christian (2007), "Toward the Simplified Design of Single-Angle Beam-Columns," *Engineering Journal*, Vol. 44, No. 1.

Hildebrand, Francis B. (1987), *Introduction to Numerical Analysis*, rev. 2nd edition, Dover Publications, New York.

Lutz, LeRoy A. (1996), "A Closer Examination of the Axial Capacity of Eccentrically Loaded Single Angle Struts," *Engineering Journal*, Vol. 33, No. 2.

Lutz, LeRoy A. (2006), "Evaluating Single-Angle Compression Struts Using an Effective Slenderness Approach," *Engineering Journal*, Vol. 43, No. 4.

Mengelkoch, N.S. and Yura, J.A. (2002), "Single-Angle Compression Members Loaded Through One Leg," *Proceedings of the Structural Stability Research Council,* Annual Technical Session.

Sakla, Sherif S. S. (2001), "Tables for the Design of Eccentrically Loaded Single Angle Struts," *Engineering Journal*, Vol. 38, No. 3.

Timoshenko, Stephen P. and Gere, James M. (1961), *Theory of Elastic Stability,* 2nd edition, McGraw-Hill, New York.

Yongcong, Ding and Madugula, Murty K. S. (2004), "Elastic and Plastic Section Moduli of Steel Angles About Principal Axes," *Engineering Journal*, Vol. 41, No. 1.

Yu, Wei-Wen (1985), *Cold-Formed Steel Design,* John Wiley and Sons, New York.

APPENDIX

EFFECTIVE SLENDERNESS RATIO OF SINGLE-ANGLE WEB MEMBERS

In this Appendix, the symbols r_x, r_y and r_z are the radii of gyration listed in the tables of dimensions of the AISC manuals.

1. Planar Trusses

For web members of planar trusses, the relevant equations are E5-1 and E5-2. For equal-leg angles ($r_u = r_x = r_y$) or unequal-leg angles connected through the long leg ($r_u = r_y$):

a. When $L/r_u \le 80$

$$\frac{KL}{r} = 72 + 0.75\frac{L}{r_u} \tag{A2-1}$$

b. When $L/r_u > 80$

$$\frac{KL}{r} = 32 + 1.25\frac{L}{r_u} \le 200 \tag{A2-2}$$

For unequal-leg angles connected through the short leg, with $\rho = b_l/b_s < 1.7$:

a. When $L/r_x \le 80$

$$\frac{KL}{r} = 72 + 0.75\frac{L}{r_x} + 4(\rho^2 - 1) \ge 0.95\frac{L}{r_z} \tag{A2-3}$$

b. When $L/r_x > 80$

$$\frac{KL}{r} = 32 + 1.25\frac{L}{r_x} + 4(\rho^2 - 1) \ge 0.95\frac{L}{r_z} \le 200 \tag{A2-4}$$

2. Box or Space Trusses

For web members of box trusses, the relevant equations are E5-3 and E5-4. For equal-leg angles ($r_u = r_x = r_y$) or unequal-leg angles connected through the long leg ($r_u = r_y$):

a. When $L/r_u \le 75$

$$\frac{KL}{r} = 60 + 0.8\frac{L}{r_u} \tag{A2-5}$$

b. When $L/r_u > 75$

$$\frac{KL}{r} = 45 + \frac{L}{r_u} \le 200 \tag{A2-6}$$

For unequal-leg angles connected through the short leg, with $\rho = b_l/b_s < 1.7$:

a. When $L/r_x \le 75$

$$\frac{KL}{r} = 60 + 0.8\frac{L}{r_x} + 6(\rho^2 - 1) \ge 0.82\frac{L}{r_z} \tag{A2-7}$$

b. When $L/r_x > 75$

$$\frac{KL}{r} = 45 + \frac{L}{r_x} + 6(\rho^2 - 1) \ge 0.82\frac{L}{r_z} \le 200 \tag{A2-8}$$